Vol.2, No.2, Page 107- 115, 2024 https://doi.org/10.59628/jast.v2i2.938 ISSN 2958-9568 JAST

SUN PUBLISHER

مجلة جامعة صنعاء للعلوم التطبيقية والتكنولوجيا

Sana'a University Journal of Applied Sciences and Technology

https://journals.su.edu.ye/index.php/jast/

Solitary waves and double layers of dust-acoustic waves propagating in a non-ideal dusty plasma

Mahmood A. H. Khaled[1] *, Kawkab A. M. Alsa'adi[1] and Ibrahim G. H Loqman[1]

[1] **Department of Physics, Faculty of Science, University of Sana'a, Sana'a, Yemen.**

*Corresponding author: mahkhaled@hotmail.com

Abstract

The dust-acoustic (DA) solitary waves and double layers structures of the dust-acoustic waves (DAWs) have been investigated in the framework of Gardner approach, in a non-ideal dusty plasma system consisting of electrons, ions and negatively charged dust grains. The non-ideal effects are examined by incorporating the van der Waals (VDW) equation of state for the dust grains. Using reductive perturbation technique, the Gardner's equation is derived. The effects of the non-ideal parameters on the profiles of solitary wave and double layer structures are discussed in some detail. It is found that the amplitude and width of both solitary waves and double layers are significantly modified by the non-ideal parameters. Also, it is shown that the wave phase velocity undergoes a significant change due to the presence of non-ideal effects in the system.

Article Info

Keywords:
Gardner equation, Double-layers, Non-ideal plasma, Solitary waves.

Article History:
Received: 28-March-2024,
Revised: 28-April-2024,
Accepted: 30-April-2024,
Available online: 5 May 2024

1. INTRODUCTION

In recent years, the study of nonlinear structures (such as solitary waves, shock waves, double layers,. . .) associated with the propagation of dust-acoustic waves (DAWs) has become one of the most important research topics in dusty plasma physics due to the important role not only in astrophysics space plasmas [1–4], but also in understanding the properties of laboratory plasmas [5, 6]. Over the years, many investigations have been carried out on the nonlinear structures of DAWs in a dusty plasma physics, especially dust acoustic (DA) solitary waves, and double layers (DLs) [7–18]. Some of these investigations were limited to the framework of Sagdeev's approach (which is valid for large amplitude solitary waves) [11–14, 16–19], while the other investigations are confined to the framework of modify Korteweg-de Vries (MKdV) equation [7, 16, 18], which is valid for small amplitude limit, but not valid for a parametric regime, in which the nonlinear term coefficient for Korteweg-de Vries (KdV) equation equal zero. [19]. Another approach is Gardner's approach which leads to the standard Gardner equation [20] that can be used to study the nature of solitary waves and DLs in a dusty plasma physics [21–25]. Mannan and Mamun [21] investigated the nonlinear propagation of cylindrical and spherical Gardner solitons in a dusty plasma having positively and negatively charged dust as well as Maxwellian electrons and ions. Also, Mamun and Mannan [22] explored nonplanar DA double layers in an opposite polarity dusy plasma in the framework of Gardner equation. Asaduzzaman and Mamun [23] derived the Gardner equation and investigated the non-planar dust-acoustic double layers in a dusty plasma having two temperature ion, Maxwellian electrons and negatively charged dust grians. Tasnim *et al.* [24] used Gardner's approach to describe DA solitary waves, and DLs in a dusty plasma system consisting of negatively charged mobile dust grains, Maxwellian electrons, and nonthermal ions of two distinct temperatures. Addition, Tasnim *et al.* [25] derived the modified Gardner's equation to investigate the cylindrical and spherical DAWs in a dusty plasma consisting of Maxwellian electrons, two temperatures nonthermal ions as well as negatively charged dust grains. However, all of the above investigations are

focused on the ideal behavior of the dust grains which is a valid approximation used in most dusty plasmas in which the size of dust grain is on the order of micrometers or less and for dilute plasmas. For dusty plasmas with larger dust grain sizes, the intergrain interactions between the neighboring dust grains becomes increasingly significant and hence, the ideal approximation breaks down and usual equation of state used to describe ideal dusty plasmas behavior has to be replaced by one that accounts for non-ideal effects. In fact, dusty plasmas usually have non-ideal behavior [26, 27]. Therefore, the aim of this paper is to investigate the DA solitary waves and DLs in a non-ideal dusty plasma system comprising of negatively charged mobile dust grains and Maxwellian electrons and ions, in the framework of extended Gardner equation.

2. THEORETICAL MODEL

We consider a one-dimensional propagation of DAWs in a non-ideal dusty plasma consisting of Boltzmann electrons, ions and negatively charged dust grains. The non-ideal effects are examined by incorporating the VDW equation of state for the dust component. From Boltzmann distribution, the number densities of electrons n_e and ions n_i are given by [28]

$$n_e = n_{e0} exp\left(\frac{e\varphi}{k_B T_e}\right), \tag{1}$$

$$n_i = n_{i0} exp\left(-\frac{e\varphi}{k_B T_i}\right), \tag{2}$$

where n_{i0} (n_{e0}) and T_i (T_e) are the unperturbed number density and temperature of ions (electrons) respectively, φ refers to electrostatic potential, e is the electron charge and k_B is Boltzmann constant. At equilibrium, the quasi-neutrality condition is $n_{i0}{=}n_{e0}{+}Z_d n_{d0}$ where n_{d0} is unperturbed dust number density and Z_d is the dust charge number. The hydrodynamic equations governing nonlinear propagation of DAWs in such non-ideal dusty plasma model are given by

$$\frac{\partial n_d}{\partial t} + \frac{\partial}{\partial x}(n_d u_d) = 0, \tag{3}$$

$$m_d n_d \left(\frac{\partial}{\partial t} + u_d \frac{\partial}{\partial x}\right) u_d = Z_d n_d \frac{\partial \varphi}{\partial x} - \frac{\partial p_d}{\partial x}, \tag{4}$$

$$\frac{\partial^2 \varphi}{\partial x^2} = \frac{e}{\epsilon_0}(n_e - n_i + Z_d n_d), \tag{5}$$

where n_d and u_d are the number density and flow velocity of dust grains respectively, while m_d represents the dust grain mass. Here, the non-ideal effects of dust grains come in through the use of the VDW equation of state [27]. Accordingly, the dust fluid pressure (p_d) in Eq. (4) can be expressed in terms of dust number density (n_d) by the VDW equation as

$$(p_d + An_d^2)(1Bn_d) = n_d k_d T_d, \tag{6}$$

where T_d is the dust temperature and $k_d{=}R_d/N_A$, N_A is the Avogadro number' and R_d is the gas constant. The coefficients A and B have their usual definitions, namely, $A{=}\ 9k_d T_c/8n_c$ and $B{=}1/n_c$, where the subscript 'c' indicating the respective values at the critical point. To simplify the governing Eqs. (1)-(6), we defining the dimensionless variables $n = n_d/n_{d0}$, $u = u_d/C_d$ $\phi = Z_d e\varphi/k_B T_0$, $P = p_d/(n_{d0}k_d T_d)$. The space and time variables normalized as $x \to x/\lambda_D$ and $t \to t\omega_{pd}$. Here, C_d, λ_D, ω_{pd} and T_0 are the DA speed, Debye length, dust plasma frequency and the effective temperature, respectively, are given by $\lambda_D = \sqrt{\epsilon_0 k_B T_0/n_{d0}Z_d^2 e^2}$, $C_d = \sqrt{k_B T_0/m_d}$, $\omega_{pd} = \sqrt{n_{d0}Z_d^2 e^2/\epsilon_0 m_d}$, and $T_0 = Z_d s\ T_i$ where $s{=}(1-\delta)/(1+\sigma\delta)$. Therefore, the basic Eqs. (3)-(5) can be rewritten in the following normalized form

$$\frac{\partial n}{\partial t} + \frac{\partial}{\partial x}(nu) = 0, \tag{7}$$

$$n\left(\frac{\partial}{\partial t} + u\frac{\partial}{\partial x}\right)u = n\frac{\partial \phi}{\partial x} - \beta\frac{\partial P}{\partial x}, \tag{8}$$

$$\frac{\partial^2 \phi}{\partial x^2} = \rho, \tag{9}$$

$$\rho = n + \frac{1}{1-\delta}\left[\delta \exp(\sigma s\phi) - \exp(-s\phi)\right]. \tag{10}$$

From Eq. (6) we can get the following normalized equation of state

$$\frac{\partial P}{\partial x} = \frac{9}{4}\left[\frac{4}{(3-\alpha n)^2} - \alpha\theta_c n\right] \tag{11}$$

where $\beta = k_d T_d/k_B T_0$, $\alpha = n_{d0}/n_c$, $\theta_c = T_c/T_d$, $\sigma = T_i/T_e$, $\delta = n_{e0}/n_{i0}$. Now, we assume that the normalized potential ϕ is small, such that $\phi \ll 1$. As a consequence of this, the exponential functions appearing in Eq. (10) can be expanding as $\exp(j\phi) = 1{+}J\phi + (J\phi)^2/2{+}(J\phi)^3/6{+}\ldots$. Therefore, Eq. (10) simplifies to

$$\rho = n{-}1{+}c_1\phi{+}c_2\phi{+}c_3\phi^3{+}\ldots, \tag{12}$$

where the coefficients c_1, c_2 and c_3 are calculated to be

$$c_1 = 1, \quad c_2 = \frac{(1-\delta)(\delta\sigma^2 - 1)}{2(1+\delta\sigma)^2},$$

$$c_3 = \frac{(1-\delta)^2(\delta\sigma^3 + 1)}{6(1+\delta\sigma)^3}.$$

3. DERIVATION OF THE GARDNER EQUATION

To derive the Gardner equation that governing behavior of DAWs in such non-ideal dusty plasma system, we employ the well known standard reductive perturbation technique (RPT) [19]. Accordingly, the independent variables are stretched as

$$\xi = \epsilon\,(x - \lambda_0 t)\,, \quad \tau = \epsilon^3 t\,, \tag{13}$$

where λ_0 is the normalized linear phase velocity of the DAWs and ϵ is small parameter $(0 < \epsilon < 1)$ measures the strength of nonlinearity. here, the dependent physical quantities are expanded in a power series of ϵ as

$$\begin{pmatrix} n \\ u \\ \phi \\ P \\ \rho \end{pmatrix} = \begin{pmatrix} 1 \\ 0 \\ 0 \\ 1 \\ 0 \end{pmatrix} + \sum_{j=1}^{\infty} \epsilon^j \begin{pmatrix} n_j \\ u_j \\ \phi_j \\ P_j \\ \rho_j \end{pmatrix}. \tag{14}$$

Substituting Eq. (13) and Eq. (14) into the normalized basic Eqs. (7)-(12), and then equating the coefficients of different powers of ϵ. From the lowest order (i.e., ϵ) equations, the following relations are obtained

$$n_1 = -\frac{\phi_1}{\lambda_0^2 - \beta\gamma}\,, \tag{15}$$

$$u_1 = -\frac{\lambda_0 \phi_1}{\lambda_0^2 - \beta\gamma}\,, \tag{16}$$

$$P_1 = -\frac{\gamma \phi_1}{\lambda_0^2 - \beta\gamma}\,, \tag{17}$$

$$\rho_1 = n_1 + \phi_1 = 0\,, \tag{18}$$

where the coefficient γ is given by

$$\gamma = \frac{9}{4}\left[\frac{4}{(3-\alpha)^2} - \alpha\theta_c\right].$$

Substituting Eq. (15) into Eq. (18), we can obtain the normalized phase velocity of DAW as

$$\lambda_0 = \sqrt{\beta\gamma + 1}\,. \tag{19}$$

It is clear that the wave phase velocity (λ_0) is modified due to the contributions of the non-ideal effects of dust component via the non-ideal parameters β and γ.
Figure 1 shows the variation of the normalized phase velocity λ_0 of DAW with the non-ideal parameters $\alpha = n_{d0}/n_c$ and $\theta_c = T_c/T_d$, for fixed values of other parameters $\beta = 0.1$, $\delta = 0.4$ and $\sigma = 0.05$. It is obvious from this figure that for small value of $\theta_c < 1$, the phase velocity increases with increasing α parameter while for larger

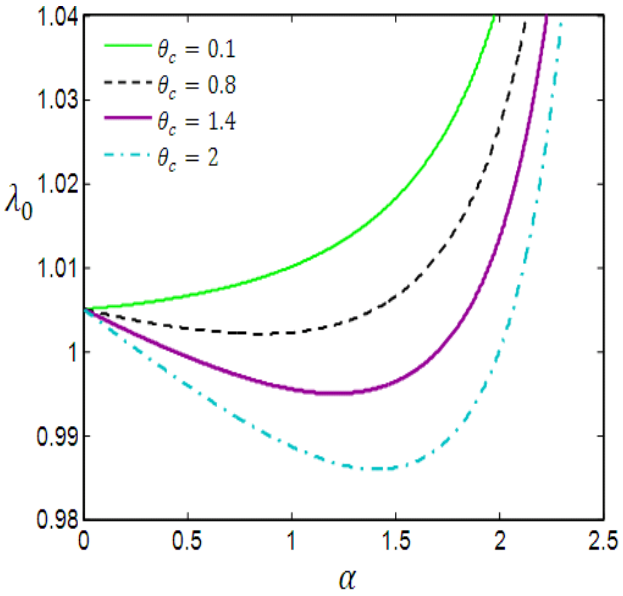

Figure 1. The normalized phase velocity λ_0 of DAW against α parameter for different values of θ_c along with $\beta = 0.01$, $\delta = 0.4$, and $\sigma = 0.05$.

values of $\theta_c \geq 1$, the values of λ_0 diminishes. Physically, this means that increasing θ_c-parameter implies a decrease in the dust temperature T_d and therefore a decrease in the thermal energy of the dust grains. As a result, the plasma becomes strongly coupled and then the effect of cohesive forces becomes dominant, which leads to a reduction in the phase velocity of DAW. But for smaller values of θ_c, the dust temperature increases, thus increasing its thermal energy. As a result, the cohesive forces are reduced and the non-ideal behavior of dust component approaches ideal behavior. In the other hand, increasing the parameter α leads to an increase in the dust number density, which reduces the volume available to dust grains for free motion. Hence the volume reduction effects are increased and the dust plasma becomes more non-ideal in nature.
Form the next order (ϵ^2) terms, we obtain the following equations

$$\frac{\partial u_2}{\partial \xi} + \frac{\partial n_1 u_1}{\partial \xi} - \lambda_0 \frac{\partial n_2}{\partial \xi} = 0\,, \tag{20}$$

$$\beta\frac{\partial p_2}{\partial \xi} - \lambda_0 \frac{\partial u_2}{\partial \xi} + u_1 \frac{\partial u_1}{\partial \xi} - \lambda_0 n_1 \frac{\partial u_1}{\partial \xi} - \frac{\partial \phi_2}{\partial \xi} - n_1 \frac{\partial \phi_1}{\partial \xi} = 0\,, \tag{21}$$

$$\frac{\partial P_2}{\partial \xi} = \gamma \frac{\partial n_2}{\partial \xi} + \gamma_1 n_1 \frac{\partial n_1}{\partial \xi}\,, \tag{22}$$

$$\rho_2 = n_2 + \phi_2 + c_2 \phi_1^2 = 0\,, \tag{23}$$

where the parameter γ_1 is given by

$$\gamma_1 = \frac{\alpha}{3-\alpha}\left[2\gamma - \frac{27}{4}\theta_c(1-\alpha)\right],$$

with the help of lowest order Eqs. (**??**)-(**??**), we solve the Eqs. (20)-(22) and obtain the following relations

$$n_2 = \frac{1}{2}(2\lambda_0^2 + \beta\gamma_1 + 1)\phi_1^2 - \phi_2\,, \tag{24}$$

$$u_2 = \frac{1}{2}\lambda_0\left(\beta\gamma_1 + 2\lambda_0^2 - 1\right)\phi_1^2 - \lambda_0\phi_2\,, \tag{25}$$

$$P_2 = \frac{1}{2}\left[\gamma\left(2\lambda_0^2\gamma + \beta\gamma_1 + 1\right) + \gamma_1\right]\phi_1^2 - \gamma\phi_2\,. \tag{26}$$

Now, substituting Eq. (24) into Eq. (23) we get

$$\rho_2 = \frac{1}{2}A\phi_1^2 = 0\,, \tag{27}$$

where A is given by

$$A = 1 + 2\lambda_0^2 + \beta\gamma_1 + 2c_2\,. \tag{28}$$

It is obvious from Eq. (27) that $\phi_1 \neq 0$ since $A = 0$ at its critical value $\beta{=}\beta_c$. The solution of $A\,(\beta{=}\beta_c) = 0$ yields the critical condition (β_c) as

$$\beta_c = -\frac{(3 + 2c_2)}{\gamma_1 + 2\gamma}\,. \tag{29}$$

So, for β around its critical value β_c, i.e., $|\beta{-}\beta_c| \equiv \epsilon$ corresponding to $A = A_0$ where A_0 is expressed by

$$A_0 \equiv \mu\left(\frac{\partial A}{\partial\beta}\right)_{\beta=\beta_c}|\beta{-}\beta_c| = \epsilon\mu A_\beta\,, \tag{30}$$

where A_β is given by

$$A_\beta = 2\gamma + \gamma_1\,. \tag{31}$$

Here, $\mu = 1$ for $\beta > \beta_c$ and $\mu{=}{-}1$ for $\beta{<}\beta_c$. Hence, when $\beta \neq \beta_c$, one an express ρ_2 as

$$\rho_2 \approx \frac{1}{2}\epsilon\mu A_\beta\phi_1^2\,. \tag{32}$$

This means that for $\beta{=}\beta_c$, ρ_2 must be within the third order Poisson's equation. Therefore, the third order (ϵ^3) Poisson's equation can be written as

$$\frac{\partial^2\phi_1}{\partial\xi^2} = n_3 + \frac{1}{2}\mu A_\beta\phi_1^2 + \phi_3 + 2c_2\phi_1\phi_2 + c_3\phi_1^3\,. \tag{33}$$

For the third order (ϵ^3) continuity and momentum equations we get:

$$\frac{\partial n_1}{\partial\tau} - \lambda_0\frac{\partial n_3}{\partial\xi} + \frac{\partial n_2 u_1}{\partial\xi} + \frac{\partial n_1 u_2}{\partial\xi} + \frac{\partial u_3}{\partial\xi} = 0\,, \tag{34}$$

$$\frac{\partial u_1}{\partial\tau} - \lambda_0\frac{\partial u_3}{\partial\xi} + \frac{\partial u_1 u_2}{\partial\xi} - \lambda_0 n_2\frac{\partial u_1}{\partial\xi} - \lambda_0 n_1\frac{\partial u_2}{\partial\xi} + n_1 u_1\frac{\partial u_1}{\partial\xi} - \frac{\partial u\phi_3}{\partial\xi} - n_1\frac{\partial\phi_2}{\partial\xi} - n_2\frac{\partial\phi_1}{\partial\xi} + \beta\frac{\partial P_3}{\partial\xi} = 0\,, \tag{35}$$

where P_3 is given by

$$P_3 = \gamma n_3 + \gamma_1 n_1 n_2 + \frac{9\alpha^2}{(3-\alpha)^4}n_1^3\,. \tag{36}$$

Eliminating u_3 between Eq. (34) and Eq. (35), using Eqs. (15)-(17), along with Eqs.(24)-(26), and then substituting into third order Poisson's equation Eq. (33) we obtain the following Gardner's equation

$$\frac{\partial\phi_1}{\partial\tau} + Q\phi_1\frac{\partial\phi_1}{\partial\xi} + R\phi_1^2\frac{\partial\phi_1}{\partial\xi} + S\frac{\partial^3\phi_1}{\partial\xi^3} = 0\,, \tag{37}$$

in which the coefficients Q, R and S are given by

$$Q = S\mu A_\beta\,, \tag{38}$$

$$R = \frac{1}{4\lambda_0}\times \left[1 + 2\lambda_0^2 + 3\left(2\lambda_0^2 + \beta\gamma_1\right)^2 + 4\beta\gamma_1 + \frac{54\alpha^2\beta}{(3-\alpha)^4} - 6c_3\right]\,, \tag{39}$$

$$S = \frac{1}{2\lambda_0}\,. \tag{40}$$

4. SOLUTIONS OF GARDNER'S EQUATION AND DISCUSSIONS

To obtain the steady-state solutions of Gardner's equation (37), we introduce the following transformations [9]

$$\eta = \xi - U_0\tau,\;\; \phi_1(\xi,\tau) = \phi_1(\eta)\,, \tag{41}$$

where η is the transformed coordinates with respect to a frame moving with velocity U_0. Using the transformations Eq. (41) into Eq. (37) and after integrating once with respect to η we obtain the following equation

$$\frac{d^2\phi_1}{d\eta^2} = \frac{U_0}{S}\phi_1 - \frac{Q}{2S}\phi_1^2 - \frac{R}{3S}\phi_1^3\,, \tag{42}$$

where the following boundary conditions were used [28]

$$\phi_1, \frac{d\phi_1}{d\eta}, \frac{d^2\phi_1}{d\eta^2} \to 0\; as\;\; |\eta| \to \pm\infty\,.$$

Multiplying Eq. (42) by $d\phi_1/d\eta$ and integrating once with using the above boundary conditions, we obtain the following energy equation

$$\frac{1}{2}\left(\frac{d\phi_1}{d\eta}\right)^2 + V(\phi_1) = 0\,, \tag{43}$$

where $V(\phi_1)$ is the Sagdeev potential (SP), is given by

$$V(\phi_1) = \frac{R}{12S}\phi_1^4 + \frac{Q}{6S}\phi_1^3 - \frac{U_0}{2S}\phi_1^2\,. \tag{44}$$

4.1. DA SOLITARY WAVES

It is clear from Eq. (44) that $V(\phi_1) = dV(\phi_1)/d\phi_1 = 0$ and $d^2V(\phi_1)/d\phi_1^2 < 0$ for $\phi_1 = 0$. Therefore, solitary wave solution of Eq. (43) exist if $V(\phi_1) = 0$ for $\phi_1 = \phi_m$.

So, we get

$$U_0 = \frac{Q}{3}\phi_{m1,2} + \frac{R}{6}\phi^2{}_{m1,2}, \tag{45}$$

and

$$\phi_{m1,2} = \phi_m \left(1 \pm \sqrt{1 + \frac{U_0}{V_0}}\right), \tag{46}$$

where $\phi_m = -Q/R$ and $V_0 = Q^2/6R$. Now, substituting Eq. (45) into Eq. (43), we get

$$\left(\frac{d\phi_1}{d\eta}\right)^2 + \vartheta\phi_1^2(\phi_1 - \phi_{m1})(\phi_1 - \phi_{m2}) = 0, \tag{47}$$

where $\vartheta = R/6S$, therefore, the solitary wave solution of Eq. (47) is given by [24,25]

$$\phi_1 = \left[\frac{1}{\phi_{m2}}\left(\frac{1}{\phi_{m2}} - \frac{1}{\phi_{m1}}\right)\cosh^2\left(\frac{\eta}{W}\right)\right]^{-1}, \tag{48}$$

where W is the width of the solitary wave, is given by

$$W = \frac{2}{\sqrt{\vartheta\phi_{m1}\phi_{m2}}}. \tag{49}$$

Here, we are explored the propagation properties of DA solitary waves in a non-ideal dusty plasma, wherein the dust component state is described by the VDW equation.

Figures 2 and 3 show the profiles of the DA solitary waves and its corresponding SP for different non-ideal parameter θ_c and for fixed other plasma parameters, $\alpha = 1$, $\beta = 0.01$, $\delta = 0.4$, $\sigma = 0.05$, and $U_0 = 0.1$. Figure 2 is plotted when $\theta_c < 1$ while Fig. 3 is plotted when $\theta_c > 1$. It is clear from Fig. 3(a) that, for all values of $\theta_c < 1$, the solitary wave amplitude is decreases with the increase of θ_c while its width becomes wider. This is also clear from Fig. 2(b) where we notice that by increasing $\theta_c < 1$, the depth of the SP decreases.

On the other hand, when $\theta_c > 1$, the solitary wave amplitude increases as θ_c increases, while its width becomes narrower as shown in the Fig. 3(a) or (b) where Fig. 3(b) show that the depth of SP becomes deeper by increasing the parameter $\theta_c > 1$. In fact, this behavior was expected because the larger values of θ_c indicates a decrease in the temperature (T_d) of dust grain, and thus its thermal energy and the result, the cohesive forces are increased and therefore, the non-ideal effect become more important.

Moreover, Fig. 4 shows the profile of DA solitary wave Fig.4(a) and its corresponding SP Fig. 4(b) for different non-ideal parameter α. It is observed that the solitary pulse amplitude increases with increasing α parameter while its width decreases. This is also observed in the Fig. 4(b), where we can see that as α increases, both the width and depth of the SP increase. Furthermore, Fig. 5 shows how the solitary wave profile (amplitude and width) is change with larger values of α. As is clear

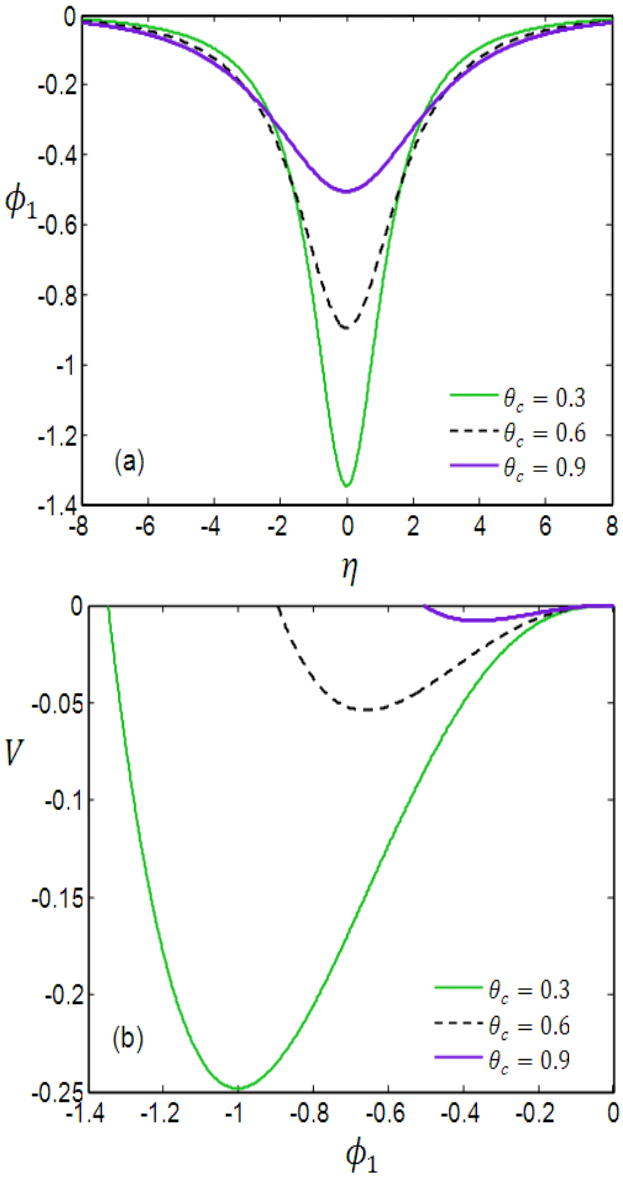

Figure 2. The profile of DA solitary wave ϕ_1 with its corresponding SP $V(\phi_1)$ for different values of $\theta_c < 1$ along with $\alpha = 1$, $\beta = 0.01$, $\delta = 0.4$, $\sigma = 0.05$, and $U_0 = 0.1$.

from this figure Fig. 5(a) or Fig. 5(b), increasing α in rang $1 \leq \alpha \leq 1.4$ leads to a solitary wave with a smaller amplitude and larger width.

On the other hand, we can notice from Fig. 5 that for all values of α-parameter that are greater than the value of θ_c-parameter (i.e., when $\alpha > 1.4$), the solitary waves amplitude (width) increases (decreases) with α-parameter. This behavior was expected because the linear phase velocity of DAW increase with the increase of α parameter in the rang $\alpha > 1.4$, but in the rang $\alpha < 1.4$, the linear phase velocity decreases with α (see Fig. 2). In fact, the increase in the α parameter indicates an increase in the number density of the dust grains (n_{d0}) which leads to reducing the volume available for free movement of dust grains. Due to the reduction of volume, the pressure is increasing, which leads to enhancing the restoring force for driving the wave travel.

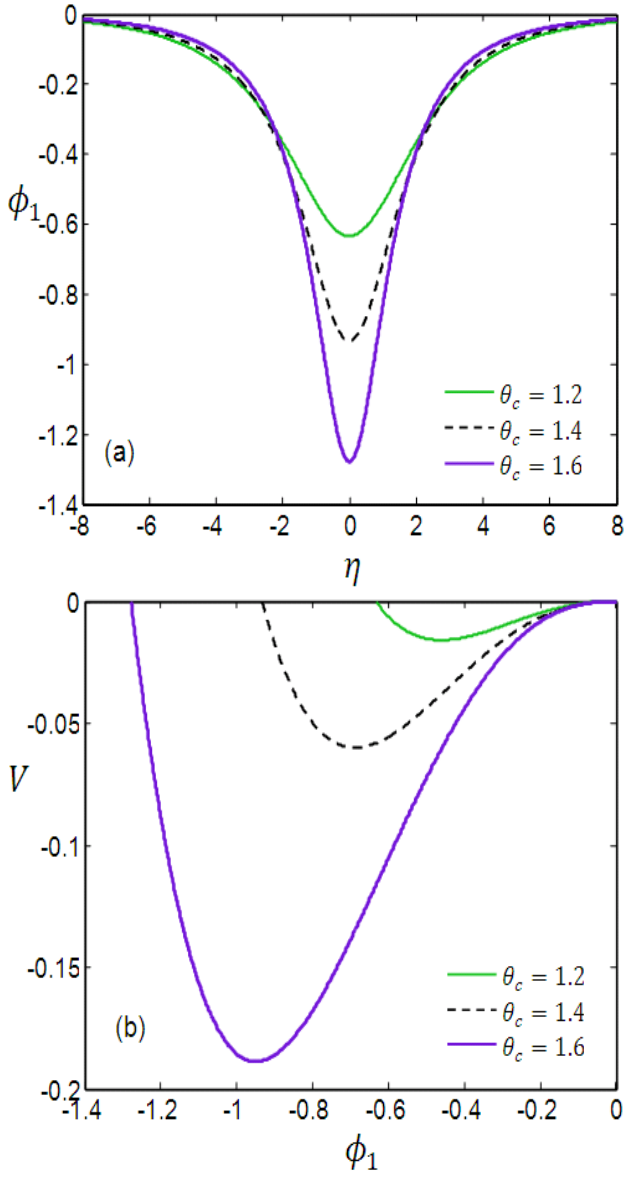

Figure 3. The profile of DA solitary wave ϕ_1 with its corresponding SP $V(\phi_1)$ for different values of $\theta_c > 1$ along with $\alpha = 1$, $\beta = 0.01$, $\delta = 0.4$, $\sigma = 0.05$, and $U_0 = 0.1$.

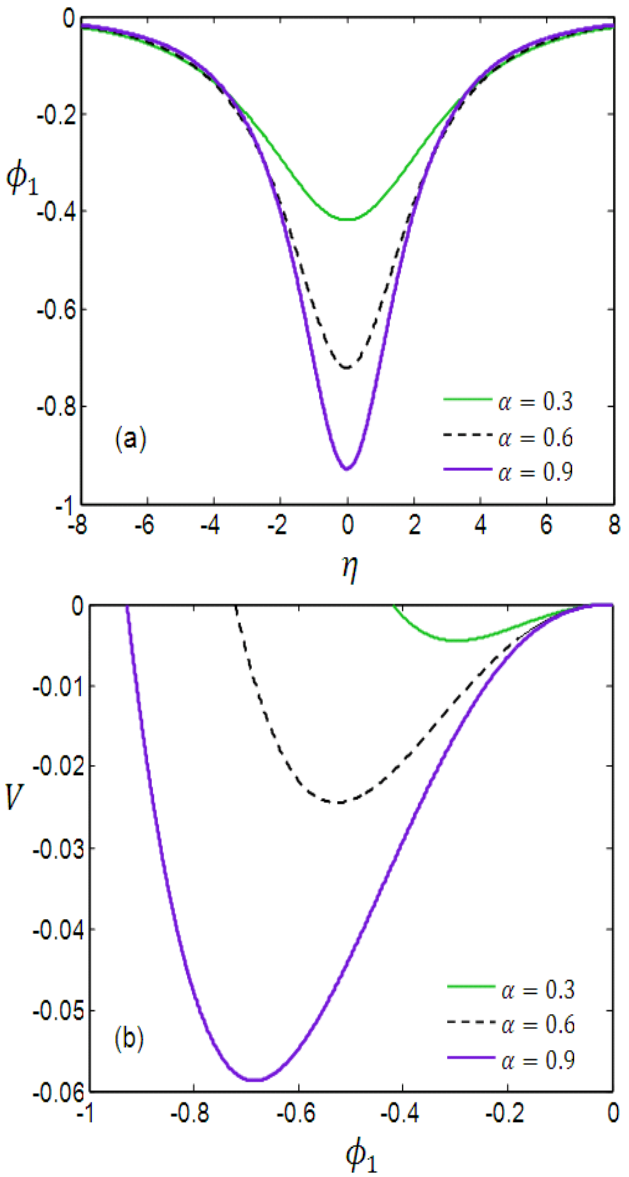

Figure 4. The profile of DA solitary wave ϕ_1 with its corresponding SP $V(\phi_1)$ for different values of $\alpha < 1$ along with $\theta_c = 1.4$, $\beta = 0.01$, $\delta = 0.4$, $\sigma = 0.05$, and $U_0 = 0.1$.

4.2. Existence of a double layers

It is important to note that, the dust acoustic double layer (DA-DL) solution of Eq. (43) requires that Sagdeev potential Eq. (44) should satisfy the following conditions:

$$V(\phi_1) = 0 \text{ for } \phi_1 = 0 \text{ and } \phi_1 = \phi_{DLm}, \quad (50)$$

$$\frac{dV(\phi_1)}{d\phi_1} = 0 \text{ at } \phi_1 = 0 \text{ and } \phi_1 = \phi_{DLm}. \quad (51)$$

Accordingly, we obtain from Eq. (44) that

$$3U_0 - Q\phi_{DLm} - \frac{R}{2}\phi_{DLm}^2 = 0, \quad (52)$$

$$2U_0 - Q\phi_{DLm} - \frac{2R}{3}\phi_{DLm}^2 = 0. \quad (53)$$

Equations (52) and (53) can be solved for propagation speed U_0 and amplitude ϕ_{DLm} of the DA-DL, resulting the propagation speed of DA-DL is

$$U_0 = -\frac{1}{6}R\phi_{DLm}^2, \quad (54)$$

while its amplitude is

$$\phi_{DLm} = -\frac{Q}{R}. \quad (55)$$

Therefore, energy equation (43) can be taken the following form

$$\frac{1}{2}\left(\frac{d\phi_1}{d\eta}\right)^2 + \frac{R}{12S}\phi_1^2(\phi_{DLm} - \phi_1) = 0, \quad (56)$$

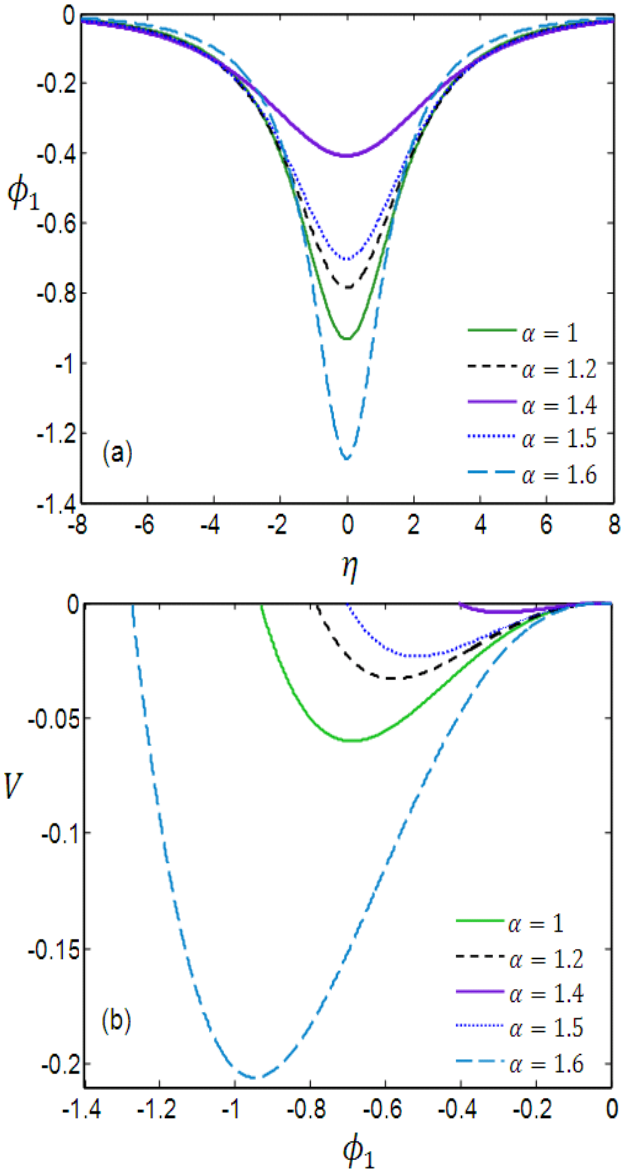

Figure 5. The profile of DA solitary wave ϕ_1 and its corresponding SP $V(\phi_1)$ for different values of $\alpha >= 1$ along with $\theta_c = 1.4$, $\beta = 0.01$, $\delta = 0.4$, $\sigma = 0.05$, and $U_0 = 0.1$.

which admits the following DA-DL solution

$$\phi_1(\eta) = \frac{1}{2}\phi_{DLm}\left[1 - \tanh\left(\frac{\eta}{W_{DL}}\right)\right], \qquad (57)$$

where W_{DL} is the width of the double layers

$$W_{DL} = \sqrt{-6S/R\phi_{DLM}^2}. \qquad (58)$$

As is clear from Eq. (58), the DA-DL structures in such non-ideal dusty plasma exist only whenever the condition $R/S < 0$ is satisfied. It is noticed from Eq. (40) that the coefficient S is always positive which leads to the higher nonlinear coefficient R, given by Eq. (39) should be negative $(R < 0)$ for the existence of DA-DL structures. Here, we have numerically analyzed the sign of higher nonlinear coefficient R to obtain the plasma parameters for the existence of DL structures in such non-ideal plasma. Figure 6 shows the contour plot of the coefficient R of higher nonlinear term in the $(\alpha,\ \theta_c)$ space. It is seen from Fig. 6 that the curve $R = 0$ divides the space $(\alpha\ ,\ \theta_c)$ into two regions: one is the region in which the value of R is positive $R > 0$, which lead to the formation of solitary pluses (no double layers formed in this region). The other one is the region in which $R < 0$ for which values of plasma parameters lead to the formation of DA-DL structures.

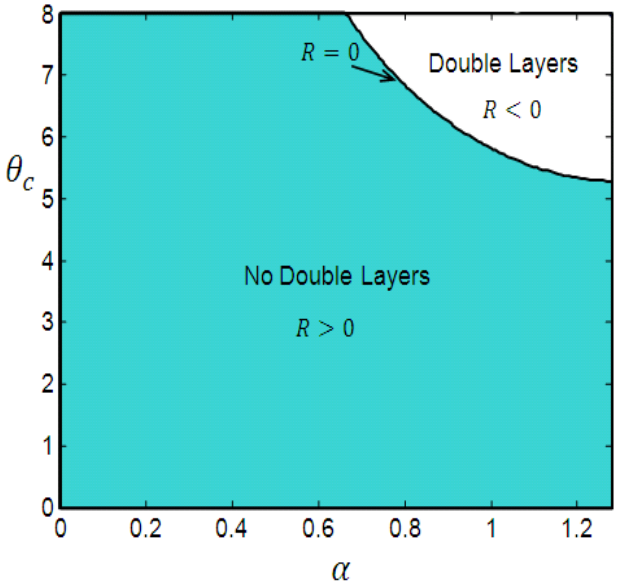

Figure 6. Contour plot of the nonlinear R coefficient in the $(\alpha\ ,\ \theta_c)$ space along with, $\beta = 0.05$, $\sigma = 0.05$ and $\delta = 0.4$.

The type of the DA-DL structure depends on the sign of coefficient Q in the expression of ϕ_{DLm} (i.e., Eq. (56)). If $Q > 0$, then ϕ_{DLm} becomes negative and a rarefactive DA-DL is formed, while for all values of $Q < 0$, the ϕ_{DLm} becomes positive and compressive DA-DL structures are obtained.

Figures 7(a) and 7(b) show the DA-DL structures and its corresponding SP respectively, for different values of non-ideal parameter θ_c. It can be seen from these figures that, only negative DL structure can be formed. The DL structures exist only between two limited values of ϕ_1. One value is fixed at $\phi_1 = 0$, while the other is at $\phi_1 = \phi_{DLm}$depending on the value of a non-ideal parameter θ_c (see Fig. 7). Figure 7(a) or 7(b) shows that the amplitude of the DA-DL structure is decreased with the increase in θ_c. Also, Fig. 7(b) indicates that the depth of the SP is decreased with the increase in θ_c-parameter, which means that the DL width increases with θ_c.

In Fig. 8 we plot the DA-DL structures and its corresponding SP for the different values of non-ideal parameter α, in the ring $0.85 \leq \alpha \leq 1$ and for fixed values for other plasma parameters as $\beta = 0.05$, $\theta_c = 7$, $\sigma = 0.05$ and $\delta = 0.4$. From this figure we can notice that the amplitude of DA-DL decreases with the increase in α-parameter. It is also found that the effect of increas-

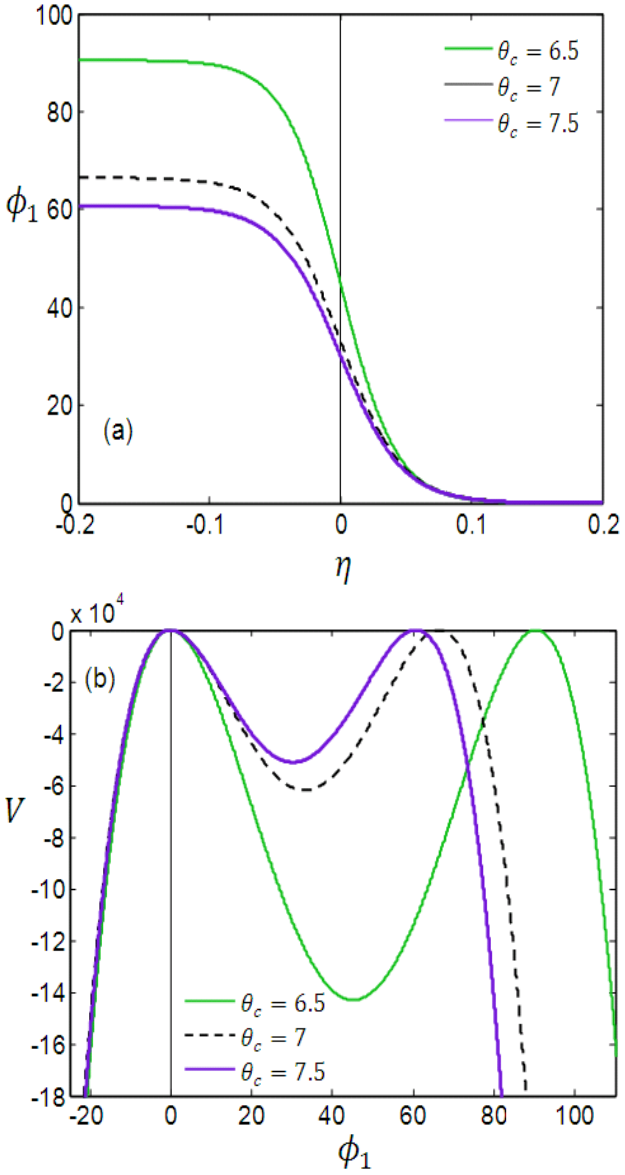

Figure 7. The profile of the DA- DL structures with its corresponding SP for different θ_c values along with $\beta = 0.05$, $\alpha = 1$, $\sigma = 0.05$ and $\delta = 0$.

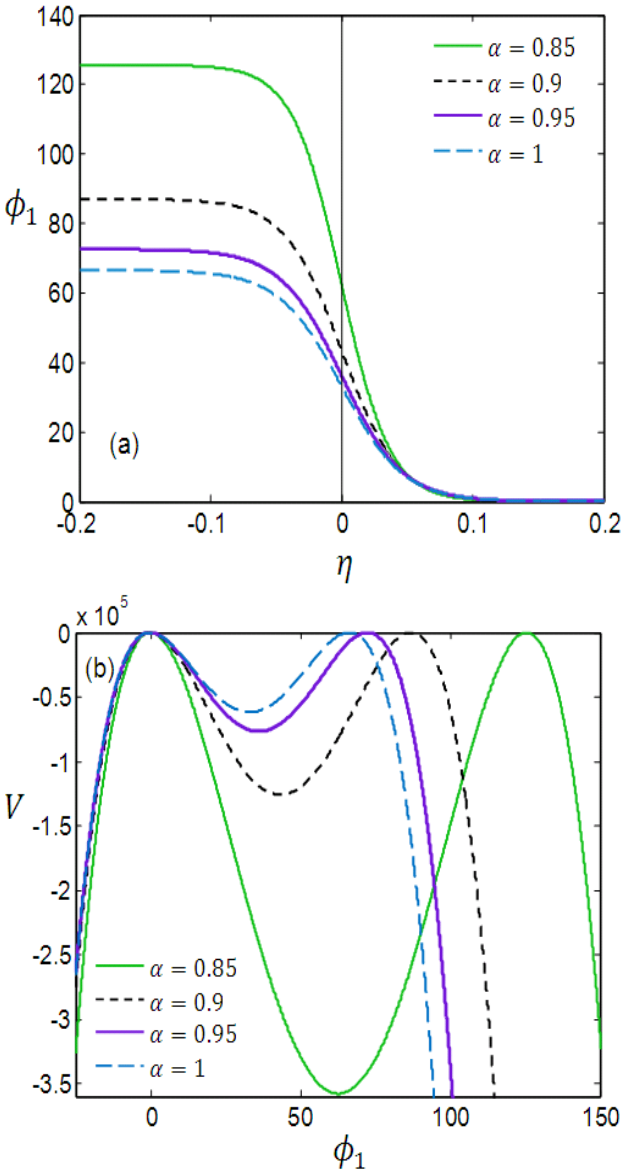

Figure 8. The profile of the DA- DL structures with its corresponding SP for different α values along with $\beta = 0.05$, $\theta_c = 7$, $\sigma = 0.05$ and $\delta = 0.4$

ing α-parameter leads to enhancing of DA-DL width as shown in Fig. 8(b) via decreasing of SP depth. Physically, increasing non-ideal parameter α means enhancing the number density of dust grains n_{d0}, which leads to reducing the volume available for dust free travel, and as a result, the non-ideal behavior of the dusty plasma becomes more dominant. This is seen to be most significant for the DA-DL structure. Moreover, the SP profile of the DL is shown in Fig. 9 for different values of δ parameter. It is observed that the amplitude of negative DL increases with the increase of δ, but its width becomes narrower.

5. CONCLUSION

The Gardner's approach has been employed to investigate the DA double layers in a non-ideal dusty plasma system comprising of electrons, ions and negatively charged dust grains. The non-ideal effects of dust grains are modeled by VDW equation of state. The RPT was used to derive the Gardner equation that describes the nature of the DA solitary waves and DLs in the current non-ideal plasma model. The solutions of Gardner equation have been used to explore the properties of the solitary waves and double layers of dust acoustic waves. The existence regions for solitary waves and double layers have been explored numerically. The combined effects of the non-ideal parameters on DA solitary waves and double layer are discussed. It is found that the widths and amplitudes of both solitary waves and DLs are affected significantly by non-ideal parameters.

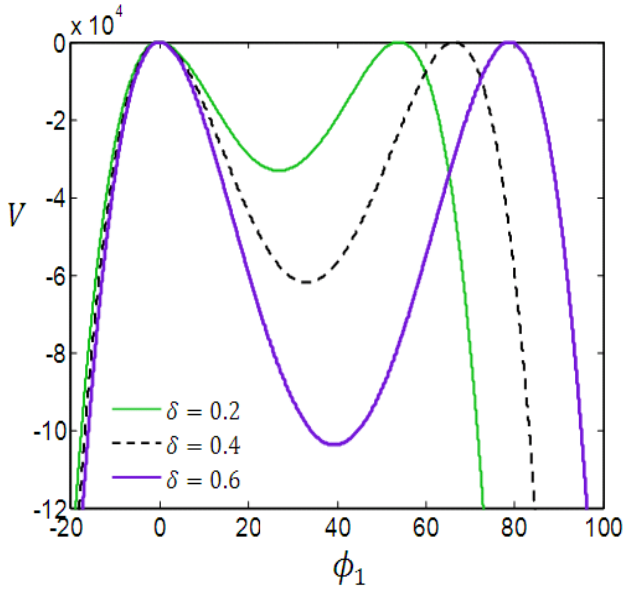

Figure 9. The profile of the dust-acoustic DL structures for different δ values along with $\beta = 0.05$, $\alpha = 1$, $\theta_c = 7$, and $\sigma = 0.05$

REFERENCES

[1] P. K. Shukla and A. A. Mamun, *Introduction to Dusty Plasma Physics* (Institute of Physics Publishing, Bristol, 2002).

[2] P. K. Shukla and B. Eliasson, "Colloquium: Fundamentals of dust-plasma interactions," Rev. Mod. Phys. **81**, 25–44 (2009).

[3] G. E. Morfill and A. V. Ivlev, "Reviews of modern physics," Rev. Mod. Phys. **81**, 1353 (2009).

[4] M. A. H. Khaled, M. A. Shukri, and Y. A. A. Hager, "Dust acoustic solitons in an opposite polarity dusty plasma in the presence of generalized polarization force," Phys. Plasmas **26**, 103702 (2019).

[5] K. E. Lonngren, "Soliton experiments in plasmas," Plasma Phys. **25**, 943 (1983).

[6] C. A. Charles, "Review of recent laboratory double layer experiments," Plasma Sources Sci. Technol. **16**, R1–R25 (2007).

[7] S. K. El-Labany, W. F. El-Taibany, A. A. Mamun, and W. M. Moslem, "Dust acoustic solitary waves and double layers in a dusty plasma with two-temperature trapped ions," Phys. Plasmas **11**, 926–933 (2004).

[8] S. K. El-Labany and W. F. El-Taibany, "Dust acoustic solitary waves and double layers in a dusty plasma with trapped electrons," Phys. Plasmas **10**, 4685–4695 (2003).

[9] S. K. El-Labany and W. F. El-Taibany, "Effect of dust-charge variation on dust acoustic solitary waves in a dusty plasma with trapped electrons," J. Plasma Phys. **70**, 69–87 (2004).

[10] W. F. El-Taibany and R. Sabry, "Dust-acoustic solitary waves and double layers in a magnetized dusty plasma with nonthermal ions and dust charge variation," Phys. Plasmas **12**, 082302 (2005).

[11] R. Bharuthram, M. Djebli, and S. R. Pillay, "Electrostatic nonlinear waves in a dusty plasma with positive dust grains and two electron species," J. plasma Phys. **72**, 35–41 (2006).

[12] F. Verheest, "Nonlinear acoustic waves in nonthermal plasmas with negative and positive dust," Phys. Plasmas **16**, 013704 (2009).

[13] B. Das, D. Ghosh, and P. Chatterjee, "Large-amplitude double layers in a dusty plasma with an arbitrary streaming ion beam," Pra-mana. J. Phys. **74**, 973–981 (2010).

[14] H. Marif and M. Djebli, "On existence conditions of dust-acoustic solitary waves in a plasma with positively charged dust," Astrophys. Space Sci. **337**, 605–611 (2012).

[15] H. Marif and M. Djebli, "On existence conditions of dust-acoustic solitary waves in a plasma with positively charged dust," Astrophys. Space Sci. **337**, 605–611 (2012).

[16] N. S. Saini and R. Kohli, "Dust-acoustic solitary waves and double layers with two temperature ions in a nonextensive dusty plasma," Astrophys. Space Sci. **348**, 483–494 (2013).

[17] M. K. Mahanta, R. Moulick, and K. S. Goswami, "Studies of dust acoustic double layers in the presence of trapped particles," J. Korean Phys. Soc. **64**, 232–237 (2014).

[18] M. A. H. Khaled, M. A. Shukri, and Y. A. A. Hager, "Large-amplitude dust acoustic solitons in an opposite polarity dusty plasma with generalized polarization force," Chin. Phys. B **31**, 010505 (2022).

[19] H. Washimi and T. Taniuti, "Propagation of ion-acoustic solitary waves of small amplitude," Phys. Rev. Lett. **17**, 996 (1966).

[20] J. A. Desanto, *Mathematical and numerical aspects of wave propagation* (SIAM, Philadelphia, 1998).

[21] A. Mannan and A. A. Mamun, "Nonplanar dust-acoustic gardner solitons in four component dusty plasma," Phys. Rev. E **84**, 026408 (2011).

[22] A. A. Mamun and A. Mannan, "Nonplanar double layers in plasmas with opposite polarity dust," JETP Lett. **94**, 356–361 (2011).

[23] M. Asaduzzaman and A. A. Mamun, "Non-planar gardner double layers in two-ion temperature dusty plasma," J. plasma phys. **78**, 601–606 (2012).

[24] I. Tasnim, M. Masud, M. Asaduzzaman, and A. A. Mamun, "Dust-acoustic gardner solitons and double layers in dusty plasma with nonthermally distributed ions of two distinct temperatures," Chaos **23**, 013147 (2013).

[25] I. Tasnim, M. M. Masud, and A. A. Mamun, "Cylindrical and spherical dust-acoustic gardner solitons in dusty plasmas with non-thermal ions of distinct temperature," Korean Phys. Soc. J. **64**, 987–993 (2014).

[26] V. E. Fortov and I. T. Iakubov, *Physics of non-ideal Plasmas* (Hemisphere, New York, 1990).

[27] N. N. Rao, "Dust-acoustic kdv solitons in weakly non-ideal dusty plasmas," Phys. Scr. T75 **1998**, 179–181 (1998).

[28] I. G. Luqman, M. A. H. Khaled, and K. I. Alkuhlani, "Quantum effects on cylindrical dust-ion acoustic waves in a semiclassical dense dusty plasma," Sana'a Univ. J. Appl. Sci. Technol. **1**, 93–102 (2023).